

See discussions, stats, and author profiles for this publication at: <https://www.researchgate.net/publication/277499609>

Molecular Size of Asphaltene Solubility Fractions

ARTICLE *in* ENERGY & FUELS · MARCH 2003

Impact Factor: 2.79 · DOI: 10.1021/ef010239g

CITATIONS

69

READS

10

6 AUTHORS, INCLUDING:



Oliver C Mullins

Schlumberger Limited

245 PUBLICATIONS 5,976 CITATIONS

SEE PROFILE



Semih Eser

Pennsylvania State University

124 PUBLICATIONS 1,259 CITATIONS

SEE PROFILE



Jonathan Paul Mathews

Pennsylvania State University

104 PUBLICATIONS 944 CITATIONS

SEE PROFILE

Molecular Size of Asphaltene Solubility Fractions

Henning Groenzin* and Oliver C. Mullins

Schlumberger-Doll Research, Old Quarry Road, Ridgefield, Connecticut 06877

Semih Eser, Jonathan Mathews, Ming-Gang Yang, and Daniel Jones

Department of Energy and Geo-Environment, Engineering, Pennsylvania State University,
University Park, Pennsylvania 16802

Received September 26, 2001

A fluorescence depolarization technique was used to determine the molecular size of asphaltene solubility fractions of a petroleum resid asphaltene. The molecular size was determined at different emission wavelengths for each solubility fraction. For each subfraction the range of molecular size was found to vary considerably. However, at a given emission wavelength, the molecular sizes for the different asphaltene solubility subfractions are very similar, that is the subfractions differ from each other by different population distributions of the same set of molecules. The size variation among the different subfractions is due to the different molecular population distributions of the constituent components. The population distribution was estimated from published LDMS results.

Introduction

Asphaltenes are the most aromatic fraction of crude oil.^{1–4} They are defined in terms of their solubility in various organic solvents. Two common but not exclusive definitions are as the crude oil fraction soluble in toluene, insoluble in *n*-heptane, or as the fraction soluble in toluene, insoluble in *n*-pentane. These definitions are very practical because they capture the heaviest end of crude oil. However, they make the complete definition of their molecular properties quite challenging. Asphaltenes have been subject of investigation by a wide variety of techniques due to their strong impact on crude oil production, transportation and refining. In general asphaltenes increase the cost in production and processing of crude oil. This is of growing concern as sources of low-asphaltene content oils, or light oils, are selectively depleted, leaving heavy oils in many remaining reservoirs.

One of the most important concerns to be addressed are the aggregative properties of asphaltenes as they have a direct impact on the production of crude oil. X-ray,⁵ neutron,^{1,6,7} and optical scattering methods^{8–10}

have successfully uncovered systematical aggregation behavior in asphaltenes. XANES and XPS spectroscopy have been utilized in determining bonding characteristics of the heteroatomic fraction, mainly sulfur^{11–13} and nitrogen¹⁴ and also carbon¹⁵ in asphaltenes.

However the molecular weight of asphaltene has been a controversial issue over the past 20 years. Various measurements have yielded results differing by an order of magnitude or more. While field ionization mass spectrometry indicates a average molecular weight of around 700 amu,¹⁶ vapor pressure osmometry favors molecular weights of around 4000 amu and size exclusion chromatography yield average molecular weights of approximately 10000 amu.¹⁷ Recent laser desorption mass spectrometry investigations have determined the asphaltene molecular weights to be in the range of 200–1200 amu.^{18,19} Nevertheless, as we discuss herein, molecular weight determination via some mass spectral

* Corresponding author. Present address: Department of Chemistry, Tufts University, Medford, MA 02155.

(1) Mullins, O. C.; Sheu, E. Y., Eds. *Structure and Dynamics of Asphaltenes*; Plenum Press: New York, 1998.

(2) Chilingarian, G. V.; Yen, T. F., Eds. *Bitumens, Asphalts and Tar Sands*. Elsevier Scientific Publishing Co.: New York, 1978.

(3) Bunger, J. W.; Li, N. C., Eds. *Chemistry of Asphaltenes*. American Chemical Society: Washington, DC, 1981.

(4) Sheu, E. Y.; Mullins, O. C., Eds. *Asphaltenes: Fundamentals and Applications*; Plenum Publishing Co.: New York, 1995.

(5) Pollack, S. S.; Yen, T. F. *Anal. Chem.* **1970**, *42*, 623.

(6) Sheu, E. Y. *Phys. Rev. A* **1992**, *45*, 2428.

(7) Ravey, J. C.; Decouret, G.; Espinat, D. *Fuel* **1988**, *67*, 1560.

(8) Anisimov, M. A.; Yudin, I. K.; Nikitin, V.; Nikolaenko, G.; Chernoustan, A.; Toulhoat, H.; Frot, D.; Briolant, Y. *J. Phys. Chem.* **1995**, *99*, 9576.

(9) Joshi, N. B.; Mullins, O. C.; Jamaluddin, A.; Creek, J.; McFadden, J. *Energy Fuels* **2001**, *15*, 979.

(10) Buckley, J. S.; Hirasaki, G. J.; Liu, Y.; Von Drasek, S.; Wang, J.-X.; Gill, B. S. *Pet. Sci. Tech.* **1998**, *16*, 251.

(11) George, G. N.; Gorbaty, L. L. *J. Am. Chem. Soc.* **1989**, *111*, 3182.

(12) Waldo, G. S.; Mullins, O. C.; Penner-Hahn, J. E.; Cramer, S. P. *Fuel* **1992**, *71*, 53.

(13) Kelemen, S. R.; George, G. N.; Gorbaty, M. L. *Fuel* **1990**, *69*, 939.

(14) Mitra-Kirtley, S.; Mullins, O. C.; van Elp, J.; George, S. J.; Chen, J.; Cramer, S. P. *J. Am. Chem. Soc.* **1993**, *115*, 252.

(15) Bergmann, U.; Mullins, O. C.; Cramer, S. P. *Anal. Chem.* **2000**, *72*, 2609.

(16) Boduszynsky, M. M. In *Chemistry of Asphaltenes*; Bunger, J. W.; Li, N. C., Eds.; American Chemical Society: Washington, DC, 1981; Chapter 7.

(17) Anderson, S. I. *Fuel Sci. Technol. Int.* **1994**, *12*, 51.

(18) Miller, J. T.; Fisher, R. B.; Thiagarajan, P.; Winans, R. E.; Hunt, J. E. *Energy Fuels* **1998**, *12*, 1290.

(19) Yang, M.-G.; Eser, S. Presented at the American Chemical Society Meeting, New Orleans. In *ACS Division of Fuel Chemistry Preprints*; American Chemical Society: Washington, DC, 1999; Vol. 44, p 768.

techniques can be problematic due to the unknown contribution of a structureless curved baseline to the overall mass spectrum of asphaltenes.

Fluorescence depolarization (FD) is a technique which is capable of directly measuring the molecular size of asphaltenes in very dilute solutions.^{20,21} Thus it is not subject to the problem of aggregation as other techniques are. In addition, fragmentation is not a concern. FD model compound analyses^{20,21} and correspondingly theoretical analysis on molecular diameters support molecular weights in the range of 400–1000 amu. The FD results on asphaltene molecular weight have been combined with ¹³C NMR and IR results to explain the difference in mass obtained for coal versus petroleum asphaltenes.²² The conclusion reached herein on the importance of van der Waals interactions of fused aromatic rings versus alkane steric interaction are supported by HRTEM results.²³

In this paper we determine the rotational correlation times τ_r (thus molecular size) for a series of six solubility fractions of a single vacuum resid crude oil. The sizes of the molecules were measured for each solubility fraction at six different emission wavelengths spanning the fluorescence emission spectrum of those solubility fractions. These results were also compared to published LDMS results on the same samples. We find that the solubility fractions vary significantly in size for different sets of excitation and emission wavelengths. However, at a given fluorescence emission wavelength, the variations among the solubility fractions is quite small. These results support the conclusion that different solubility fractions consist of similar molecular components but in different population ratios.

Experimental Section

Sample Preparation. The sample preparation has been described in detail previously.¹⁹ The basic preparation steps shall be repeated here. A vacuum residue sample was separated into *n*-pentane soluble maltenes and *n*-pentane asphaltenes. The asphaltene fraction (AS) was split into solubility fractions by separating the least soluble fractions first. The asphaltene was dissolved in toluene. After addition of *n*-pentane in a 55/45 pentane/toluene volume-ratio the insolubles were filtered. Both the precipitate and the filtrate were dried/evaporated. The precipitate was labeled the AS6 subfraction of the asphaltene. The remaining asphaltenes of the evaporated filtrate were subject to the same procedure while varying the pentane/toluene ratio to 65/35 (AS5), 75/25 (AS4), 85/15 (AS3), and 95/5 (AS2), respectively. The solvents of the remaining filtrate are evaporated and the residue is classed as AS1. The most soluble asphaltene subfraction AS1 appears more "shiny" than the subfraction AS6 and the other subfractions have a dull black color. In a similar way, *n*-pentane asphaltenes tend to be shinier than *n*-heptane asphaltenes. The way the asphaltene fraction AS was prepared, it is possible that it includes a small fraction that is not soluble in toluene and is incorporated in AS6. Typical concentrations for use in the fluorescence depolarization experiments is 0.006 mg/liter.

Fluorescence Depolarization. The seven samples were analyzed by fluorescence depolarization (FD). FD is a technique that allows direct determination of the size of a fluoro-

Table 1. Fluorescence Depolarization Decay Times for an Oblate Spheroid with a Aspect Ratio n with Respect to a Spherical Rotator and Practically used Correction Factor $C^{(n)}$ for the Transition from Spherical Model to Oblate Spheroid, Assuming Only One Exponential Decay for the Oblate Spheroid^a

| $n = 1/\rho$ | τ_1/τ_r | τ_2/τ_r | τ_3/τ_r | $C^{(n)}$ | a/r |
|--------------|-----------------|-----------------|-----------------|-----------|-------|
| 2 | 1.13 | 1.17 | 1.30 | 1.41 | 1.124 |
| 4 | 1.84 | 1.90 | 2.1 | 2.25 | 1.211 |
| 6 | 2.65 | 2.71 | 2.93 | 3.09 | 1.248 |
| 8 | 3.47 | 3.54 | 3.77 | 3.94 | 1.266 |
| 10 | 4.3 | 4.38 | 4.62 | 4.89 | 1.269 |

^a The last column compares the ratio of derived radii for an oblate spheroid (semimajor axis) vs a sphere for the same τ_r .

phore in solution and has been described in detail previously.^{20,21} For this technique, polarized time-dependent fluorescence decay curves are collected, one for each of the four possible polarization combinations of excitation and detection, labeled as vv (vertical polarization of the excitation source–vertical polarization of fluorescence emission), hv (horizontal–vertical), vh (vertical–horizontal), and hh (horizontal–horizontal). The terms vertical and horizontal in this case refer to a laboratory reference frame. All samples are run in toluene with a viscosity of 0.56 cp at room temperature at a concentration of ≈ 0.006 g/L which corresponds to an optical density of 0.2 at 337 nm for a 10 mm path length.

The spectra were taken utilizing a C-72 fluorescence lifetime spectrometer with optional A-720 steady-state attachment, made by Photon Technology International. The heart of the fluorescence lifetime system is a nitrogen laser-dye laser combination, capable of producing pulses that allow for a resolution of down to approximately 100 ps. FD measurements were performed for six different emission wavelengths, spanning the steady-state emission range of the asphaltene solubility fractions. The excitation wavelength is chosen to be ≈ 40 nm shorter than the emission.¹

To correlate chromophore size to molecular size, a measurement of the absolute size of the molecule, containing the chromophore, is necessary. The technique of fluorescence depolarization provides such a measurement. The fluorescence polarization decay time or rotational correlation time (τ_{rct} or τ_r) is directly related to the volume of the molecule. As has already been published,²⁰ the conversion from τ_r to molecular volume V is given for the case of a spherical rotator by

$$\tau_r = \frac{V\eta}{kT} \quad (1)$$

where k is the Boltzmann constant, T is the temperature and η is the viscosity of the solvent. Equation 1 is derived from a relationship between the diffusion tensor and the volume of the molecule,²⁴ which is often referred to as *Stokes–Einstein Equation* of rotational diffusion. However, in all generality τ_r is not only a function of the molecular volume as equation 1 suggests but also dependent on the shape of the molecule.

In the most general case for a completely anisotropic rotator of unknown shape, analysis is difficult as τ_r breaks down into five exponential components that are independent of each other.²⁵ However, under assumption of an oblate spheroid with rotational symmetry, these five components reduce to three that are similar to each other in magnitude and collapse into a single exponent for the case of an infinitely thin disk. For the shape of an oblate spheroid it is possible to define a single shape parameter, ρ as the ratio of the short axis to the long axis of the spheroid and therefore always smaller than one. To simplify notation the aspect ratio n shall be defined as the reciprocal of ρ . Table 1 compares the three

(20) Groenzin, H.; Mullins, O. C. *J. Phys. Chem. A* **1999**, *103*, 11237.

(21) Groenzin, H.; Mullins, O. C. *Energy Fuels* **2000**, *14*, 677.

(22) Benrosto-Gonzalez, E.; Groenzin, H.; Lira-Galeana, C.; Mullins, O. C. *Energy Fuels* **2001**, *15*, 972.

(23) Sharma, A.; Groenzin, H.; Tomita, A.; Mullins, O. C. Private communication.

(24) Favro, L. D. *Phys. Rev.* **1960**, *119*, 53.

(25) Tao, T. *Biopolymers* **1969**, *8*, 609.

exponential decay times to each other for different shape parameters.

Examination of Table 1 shows that even for large shape parameter (small n) it introduces no more than 15% error upon collapsing the three exponential decays into one. The single correction factor which is introduced upon collapsing the three exponential decays into one is denoted $C^{(n)}$ and is dependent on the reciprocal n of the shape parameter. The numerical values for $C^{(n)}$ which are listed in Table 1 involve a simplification in the calculation of the parameter over the calculation of the ratios $\tau_1/\tau_r, \dots, \tau_3/\tau_r$ which has been introduced previously.^{20,25} The relation between molecular volume and the rotational correlation time is now given by

$$\tau_{r,obl} = C^{(n)} \frac{V_{obl}\eta}{kT} \quad (2)$$

Table 1 also shows that for a given measured τ_r the calculated molecular volume decreases for increasing n . In plain words, the flatter the assumed shape of the molecule is, the smaller will its calculated volume be. This is intuitively understood since τ_r is dependent on the viscous drag of the molecule. The drag is a function of the surface area of the molecule, and a sphere has of any shape the largest volume for a given surface area. However, a quick calculation shows that the predicted larger half-axis a of the oblate spheroid is larger than the radius r of a sphere calculated for the same rotational correlation time by the factor

$$\frac{a}{r} = \left(\frac{n}{C^{(n)}} \right)^{1/3} \quad (3)$$

and will grow with increasing n , despite the fact that the calculated molecular volume is decreasing. The ratio a/r is listed in Table 1 for several values of the shape parameter n . The error in radius incurred using a spherical model for an oblate spheroid with $n = 4$ is only 21%.

The magnitude of the anisotropy, which is essentially the preexponent of the anisotropy decay, was found to be between 0.27 and 0.4 for all asphaltene solubility fractions at all excitation/emission wavelength combinations, were 0.4 is theoretically the maximum value the magnitude of the anisotropy can assume.²⁵ The magnitude of the anisotropy does not contain readily extractable size information²⁶ and was also found experimentally to have a much larger error than the measurement of τ_r . The variation of the preexponent is less than a factor of 2, while the variation of the lifetime is an order of magnitude. We therefore find the preexponent ill suited to characterize the anisotropy of the molecular species under investigation.

Aspect Ratio of Asphaltene Molecules. To evaluate the aspect ratio of the molecule it is important to consider the fact, that FD measures the *hydrodynamic* volume and shape of the molecule. From polymer chemistry it is known that the alkyl chains that are part of the asphaltene molecule will fold and displace a spherical volume with a diameter of

$$h = \sqrt{Nb} \quad (4)$$

where h is the diameter of the hydrodynamical volume of one alkyl chain alone, N is the number of atoms in the chain, and b is the average bond length within the chain.²⁷ From ¹³C measurements as well as from IR measurements the average alkyl side chain length is known to be around 5–6 carbon atoms long.²⁸ With a bond length of 1.5 Å follows that the

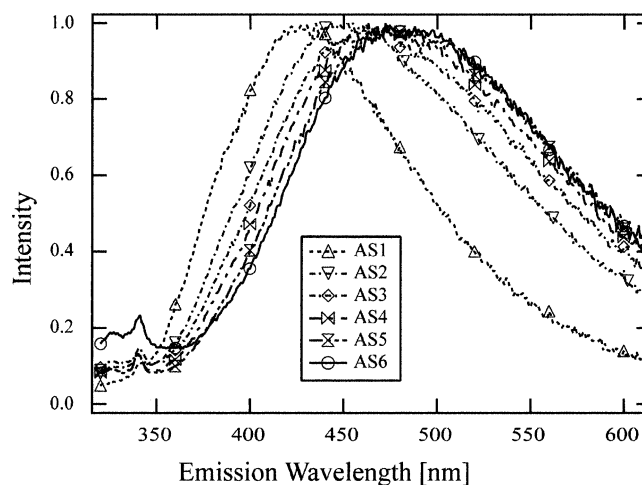


Figure 1. Steady-state spectrum of solubility fractions AS1–AS6. Samples were solved in toluene at a concentration of ≈ 0.006 g/L and excited at 310 nm. The more soluble fractions are dominated by blue-emitting chromophores which are known to be smaller than red-emitting chromophores.

average height of the asphaltene molecule can be no less than 3 Å on average. However, since in the nonaggregated state (dilute solution) the alkyl chain can still randomly “flop” around its origin (where the alkyl chain attaches to the aromatic sheet), it is actually necessary to assume a height of twice that, since the hydrodynamic sphere of the alkyl chain will randomly assume any position from completely above the aromatic sheet to completely below. It is therefore reasonable to assume a height of the molecule of at least 6 Å.

Furthermore, from previous structural analysis of asphaltene molecules,²⁹ it is reasonable to assume that the ratio of alkyl chain length/number of aromatic rings remains within a small range of values throughout the range of molecular sizes of asphaltene molecules that are spanned by a particular crude. An asphaltene molecule with a larger aromatic fraction will correspondingly have longer alkyl chains. The aspect ratio will therefore be approximately the same for all asphaltene molecules of a given crude. The stack spacing as determined by HRTEM³⁰ is ≈ 3.7 Å for petroleum asphaltene, which is consistent with the rough estimation given in the previous paragraph especially if one assumes that the flopping motion of the alkyl chains becomes impossible upon condensation of the asphaltene molecules into stacks. With the limit for the height established in the previous paragraph it is now possible to assume an aspect ratio for the asphaltene molecule, calculate a longer half-axis, and verify if the so determined smaller half-axis conforms with the independently established limit.

Results and Discussion

Figure 1 shows the steady-state spectra of the six solubility fractions of the vacuum resid (AS1–AS6). The steady-state spectrum already indicates that the fractions of lower solubility, such as AS6 contain on average larger chromophores which fluoresce at longer wavelengths than the chromophores which are contained in fractions which have a higher solubility in the binary solvent system of toluene and *n*-pentane. The correlation of fused ring size vs spectral properties has been treated in detail in reference.³¹ Generally, as expected, smaller

(26) Chuang, T. J.; Eiseenthal, K. B. *J. Chem. Phys.* 1967, 46, 5094–5097.

(27) Tobolsky, A. V.; Mark, H. F., Eds. *Polymer Science and Materials*; John Wiley & Sons: New York, 1971.

(28) Scotti, R.; Montanari, L. In *Structure and Dynamics of Asphaltenes*; Mullins, O. C.; Sheu, E. Y., Eds.; Plenum Press: New York, 1998; Chapter 3.

(29) Buenrostro-Gonzalez, E.; Anderson, S. I.; Garcia-Martinez, J. A.; Lira-Galeana, C. *Energy Fuels* 2002, 16, 732–741.

(30) Sharma, A.; Groenzin, H.; Tomita, A.; Mullins, O. C. *Energy Fuels* 2002, 16, 490–496.

(31) Ruiz-Morales, Y. *J. Phys. Chem.* Submitted for publication.

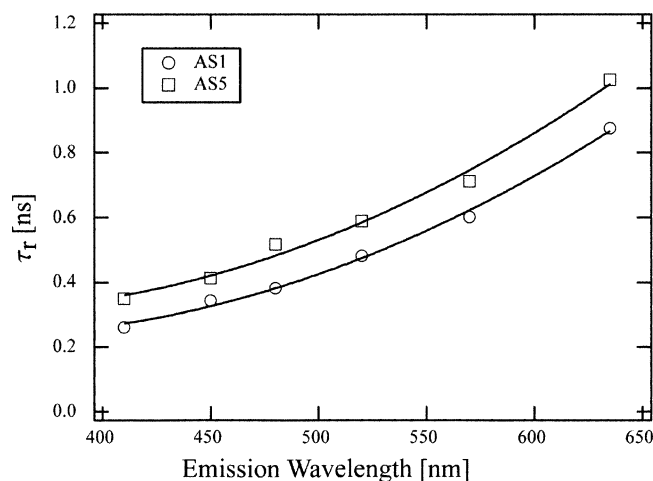


Figure 2. Rotational correlation times of two asphaltene solubility fractions for different emissions wavelengths. The correlation times are small establishing the relatively small molecular size of asphaltenes. The huge variation of molecular size with emission wavelength implies one chromophores per molecule.

ring systems fluoresce to the blue. Ring geometry can also play a major role in the optical properties of polycyclic aromatic hydrocarbons. The Raman peak at 341 nm in Figure 1 corresponds to the CH stretch mode of toluene.

Figure 2 shows the correlation of emission wavelength and molecular diameter (τ_r) for two solubility fractions AS1 and AS5. The emission wavelength is related to the chromophore size by the energy spacing of the quantum states similar to a quantum mechanical particle-in-a-box. The rotational correlation times for the two solubility fractions correspond to 9–15 Å for the longer half-axis, assuming a aspect ratio of four. This yields 4.5–7.3 Å for the height of the molecule, which agrees with the discussed lower limit for the height. If the limit is taken literally, one might even want to go to a lower aspect ratio (smaller n , more spherical shape). The case of $n = 4$ represents only a 21% correction with respect to a spherical model. One might therefore use in first approximation equation 1 to calculate the diameter of the molecule.

These considerations can be placed on even firmer ground by considering a model compound of known size and structure. Such a model compound is available as *N,N*-ditridecyl-3,4,9,10-perylene-tetracarboxylic diimide which shall be referred to in the following as “solar dye”. The FD measurements for that compound have been published previously.²⁰ According to the software CambridgeSoft ChemBats3D Pro 5.0 the distance between the two nitrogens in the optimized structure is 11.4 Å. The hydrodynamic diameter of the sphere formed by each of the two alkyl chains will be 5.4 Å, which results in a total diameter of 22.2 Å and a height of approximately 10 Å for the dye. The rotational correlation time for this dye was determined to be 0.47 ns,²⁰ which corresponds to a diameter (twice the longer half-axis of the oblate spheroid) of 20.5 Å assuming a aspect ratio of $n = 2$ and 22.1 Å assuming $n = 4$. Thus, the experimentally obtained value is in excellent agreement with the known structural information.

From further examination of Figure 2, two important features can be observed. First, with the increase of the

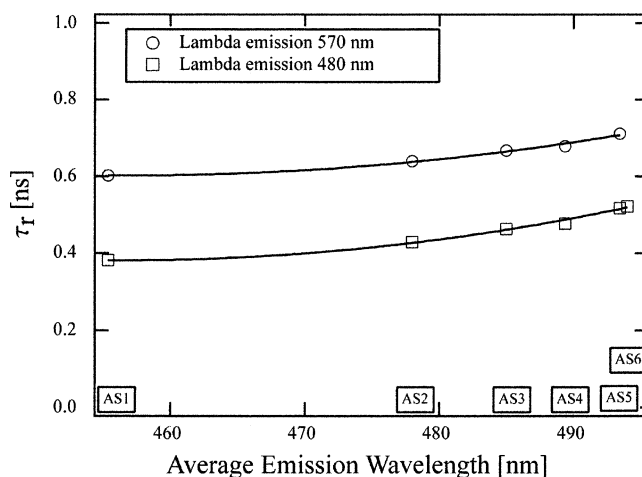


Figure 3. Rotational correlation times for two emission wavelengths as a function of average emission wavelength of steady-state spectrum (Figure 1) for all solubility fractions. For a specified emission wavelength, molecules of similar size occur in all solubility fractions.

emission wavelength and therefore the increase of the chromophore size a monotonic increase of the molecule size is observed. The increase of size with emission wavelength is very large, a factor of 4 to five here. This is only possible if there is only one chromophore per molecule. In other words, small blue-emitting chromophores are rotating much faster (by a factor of 4–5) than the large red-emitting chromophores. Thus, the blue chromophores are not tethered to the red-emitting chromophores. Thus, there is one chromophore per molecule. This implies that the selection of excitation and emission wavelength addresses selectively a subset of chromophores of a specific average size. In addition, at each emission wavelength the average molecular size is comparable for the different solubility fractions.

This is verified in Figure 3 which shows the systematic effect of decreasing solubility. Each solubility fraction is characterized by its average emission (The emission spectrum of Figure 1 is taken and each emission wavelength is weighted by its intensity. An average emission wavelength is thus obtained.) and correlated with the molecular size. Figure 3 clearly shows that within the same chromophore class as selected by the combination of excitation and emission wavelength the rotational correlation time τ_r grows monotonically for the fractions of lower solubility. However, the increase in τ_r corresponds to an increase in molecular size of only 1.9 Å, which is small compared to the increase of 7.6 Å in molecular size for the emission wavelength extremes of the same solubility fraction. The solubility effect was once evaluated at an emission wavelength close to the average emission of the solubility fractions and for confirmation of the results again at an emission wavelength at which the average size of the molecules is appreciably higher. Figures 2 and 3 are consistent with each other. The four data points: AS1, emission at 480 nm; AS1, emission at 570 nm; AS5, emission at 480 nm; and AS5, emission at 570 nm are identical in both plots. This cross-reference strongly supports the reliability of both measurements.

The relatively small variation of the rotational correlation time with the different solubility fractions at a

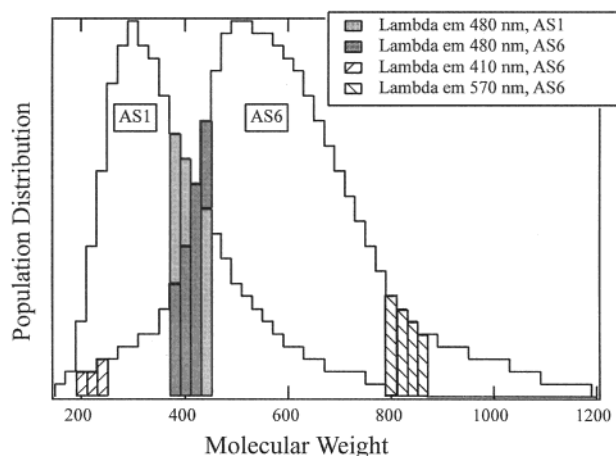


Figure 4. Schematic abundance of molecular weights in solubility fraction AS1 and AS6 as suggested by LDMS.¹⁹ Shaded areas designate range of molecular weights of molecular species in both population distributions that are emitting at 480 nm. Crosshatched areas designate range of molecular weights of molecular species that are emitting at 410 and 570 nm, respectively.

given emission wavelength (Figure 3) versus the large variation of the molecular diameter τ_r with different emission wavelengths for a given solubility fraction (Figure 2) can be explained with the help of a schematic. Figure 4 shows the schematic population distribution that according to LDMS results¹⁹ should be representative for AS1, and a schematic population distribution that should be representative for AS6.

When a mixture of several molecular species such as the solubility fractions of asphaltene is irradiated at a certain wavelength, all molecules with quantum states spaced apart less than that the energy of the irradiating light can be excited. By selecting a specific emission wavelength the number of molecules that are interrogated will be greatly reduced, though still more than one molecular species will possess an emission spectrum that contains the selected emission wavelength. These selected molecular species, however, are likely to fall into a certain range of molecular weights as the energy spacing of the quantum states can be approximated by the particle-in-the-box theory (e.g., the larger the box, the smaller the energy spacing of the quantum states). Therefore, the specification of both the excitation and emission wavelength selects a narrow range of asphaltene chromophores in terms of molecular size and weight.

As becomes immediately clear upon comparison of the two distributions in Figure 4, the statement in the previous paragraph predicts the average molecular size of the AS6 sample at a particular emission wavelength to be larger than that of the sample AS1, due to a different population distribution of molecules, but not by much. On the other hand comparing two groups of molecular species that emit at two very different wavelengths will result in a large difference in molecular size for all solubility fraction, as becomes immediately clear upon comparison of the two crosshatched areas in Figure 4. This explanation assumes that the chromophores addressed by a specific pair of excitation and emission wavelength are the same for all solubility fractions only in different ratios.

As has been stated in reference,²² the difference in the population distributions for the different solubility

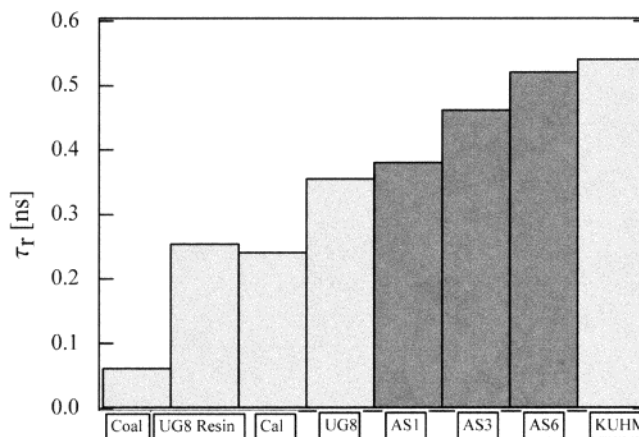


Figure 5. Rotational correlation times for different asphaltene and asphaltene solubility fractions for an emission wavelength of 480 nm. The coal asphaltene is substantially smaller due to the lack of alkanes; only small ring systems without peripheral alkanes remain soluble in toluene.²⁹ The Cal asphaltene has smaller molecules due to its high sulfoxide fraction limiting solubility.²¹

fractions can be explained by the increased interaction strength between the aromatic parts of larger asphaltene molecules which leads to a decrease in solubility. The increased interaction strength is only partially off set by the steric interaction of increased alkyl substitution. Since for a given pair of emission and excitation wavelength we observe only a small difference in size for the different solubility fractions (Figure 3) and random selection of chromophores within the different solubility fractions would give a much larger variation of size with solubility, the conclusion thus has to be, that within a particular asphaltene, the selection of both excitation and emission wavelength are tight constraints on molecular architecture.

This conclusion can be strengthened by comparison of the rotational correlation times of several asphaltene as is depicted in Figure 5. From this figure it becomes quite clear that all petroleum source materials have a similar size for a given excitation/emission pair. There are two steps in τ_r that clearly stand out in this figure. One separates the resin from the asphaltene, which is not surprising as resin has a population distribution of chromophores that is very different than that of asphaltene. The more prominent difference, however, can be observed between the coal asphaltene and the asphaltene from petroleum source material, as the chemistry for the different source materials, coal and petroleum, is different. As has been published previously,²² coal asphaltene contains smaller ring systems and shorter alkanes. In that respect, "Cal" asphaltene also stands out in that its chemical composition is peculiar.¹² "Cal" asphaltene has an unusually high alkyl sulfoxide content compared to other asphaltene, which leads to an increase of the polarity of that asphaltene. The higher polarity of asphaltene molecules is known to correlate with smaller molecular weights.³²

Figure 6 shows the correlation between LDMS molecular weights and molecular size determined by FD. The molecular weight plotted is the maximum abundance as reported in ref 19. This plot allows the direct translation from τ_r to molecular weight, which is an important result as FD only allows for the direct determination of the molecular diameter. The asphalt-

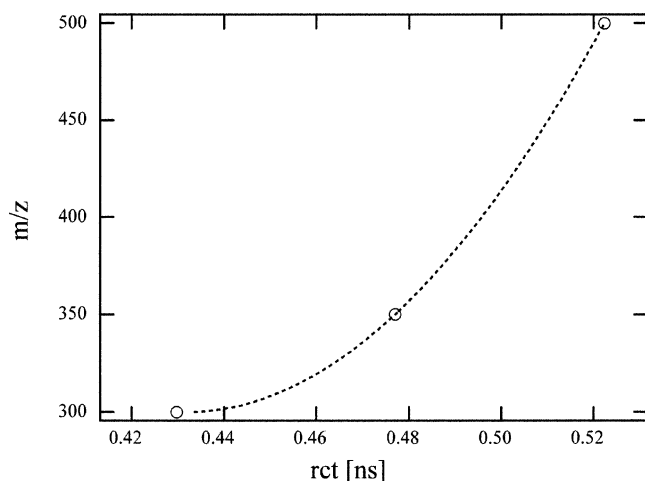


Figure 6. Correlation between τ_r (molecular diameter) and molecular weight for three selected solubility fractions.

ene solubility fractions of known molecular weight¹⁹ provide the ideal model compounds for the conversion of measured diameter τ_r to molecular weight.

It is important to note, however, that there is some uncertainty in LDMS for determination of asphaltene molecular weight because of the uncertainty in the magnitude of a large curved structureless base line in the contribution to the mass spectrum. For instance, with improper baseline subtraction, the mean asphaltene molecular weight can be incorrect easily by a factor of 5.³³ This is consistent with our findings particularly with virgin crude oil asphaltenes. We find that the

baseline issues are less important for resid asphaltenes. In particular, we find that all resolvable peaks in the LDMS spectra of all asphaltenes are less than ~ 1000 amu. These peaks ride on top of a very large baseline signal that is curved and structureless. The interpretation of this baseline peak is difficult and can lead to significant error. There is the suggestion that all of this base line in the LDMS spectra is artifact and that the peaks in the mass spectra represent the true asphaltene molecular weight.^{33,34} Work is underway to sort out mass spectral issues.³⁴

Conclusions

The molecular sizes of asphaltene solubility fractions for different excitation wavelengths were measured. We found the size of the solubility fractions to increase with decreasing solubility but only by 1.9 Å. We found a much larger variation of size with variation of excitation and emission wavelength (7.6 Å). These findings indicate that the solubility fractions all contain the same molecular species, they vary however in the ratio at which each molecular species is present in a given fraction. It appears that the solubility of a subfraction from a given source affects the population distribution but not the molecular architecture. Evidence was presented for the extension of this concept from solubility fractions of one asphaltene to the comparison of asphaltenes from different source materials. Asphaltenes of similar source material were found to have similar molecular dimensions. Asphaltenes from very different source material, such as coal asphaltenes, and asphaltenes of unusual chemical functionality were found to have different molecular sizes, too. Furthermore, the molecular size of the solubility fractions was correlated to published molecular weights determined by LDMS.

EF010239G

(32) Long, R. B. *Chemistry of Asphaltenes*; Bunger, J. W., Li, N. C., Eds.; American Chemical Society: Washington, DC, 1981; Chapter 2.

(33) Rodgers, R. Presented at the Astatphys Conference, Cancun, Mexico, 2000.

(34) Rodgers, R. Florida State University. Private communication.